Lattice-Induced Double-Valley Degeneracy Lifting in Graphene by a Magnetic Field

Igor A. Luk'yanchuk[1,2] and Alexander M. Bratkovsky[3]

[1]*University of Picardie Jules Verne, Laboratory of Condensed Matter Physics, Amiens, 80039, France*

[2]*L. D. Landau Institute for Theoretical Physics, Moscow, Russia*

[3]*Hewlett-Packard Laboratories, 1501 Page Mill Road, Palo Alto, California 94304, USA*

(Received 11 July 2007; published 2 May 2008)

We show that the recently discovered double-valley splitting of the Landau levels in the quantum Hall effect in graphene can be explained as the *perturbative* orbital interaction of intravalley and intervalley microscopic orbital currents with a magnetic field. This effect is facilitated by the translationally noninvariant terms that correspond to graphene's crystallographic honeycomb symmetry but do not exist in the relativistic theory of massless Dirac fermions in quantum electrodynamics. We discuss recent data in view of these findings.

DOI: 10.1103/PhysRevLett.100.176404 PACS numbers: 71.70.−d, 73.43.−f, 81.05.Uw

The recent discovery of massless charge carriers with linear conic spectrum, Dirac fermions (DF), in both graphite [1] and graphene [2,3] has prompted researchers to revisit many basic ideas in solid state physics based on relativistic particle physics on a lattice. The existence of Dirac fermions has been confirmed by direct angular resolved photoemission spectroscopy (ARPES) [4,5] and scanning tunneling spectroscopy (STS) [6] measurements and by Quantum Hall Effect (QHE) measurements in both graphite [7,8] and graphene [2,3]. It has been recognized that the analogy between DF in graphene and relativistic massless DF in Quantum Electrodynamics (QED) can be used fruitfully to explore the properties of graphene-based systems [9]. One of the most important consequences of this analogy is the peculiar quantization of relativistic Landau Levels (LLs) in a magnetic field that are symmetric for positive (electron) and negative (hole) energies. The LL energies are proportional $\pm\sqrt{n}$ as a function of the level number n away from the zero LL ($n = 0$) that is positioned exactly at the Dirac point where electron and hole spectra touch at zero magnetic field, $\mathbf{H} = 0$. In addition to the infinite Landau degeneracy, each level is double spin-degenerate, which is a direct consequence of the relativistic (Lorenz) invariance of the QED equations.

The QED double-spin degeneracy corresponds to the double-valley degeneracy of LLs in graphene and, together with conventional spin-degeneracy (not considered by the QED analogy), produces the conductance steps of $4e^2/h$ [10] observed in the semi-integer QHE [2,3], double the size of standard steps. Importantly, therefore, the recently discovered double-valley splitting for (at least) the zero Landau level [11,12] indicates a breakdown of relativistic invariance in graphene. Several mechanisms [13] based on *spontaneous* symmetry breaking driven by either long-range Coulomb interaction [14–18], field-enhanced electron-phonon interaction [19], disorder [20–22], or edge effects [12,23,24] have been proposed to explain this phenomenon.

In this Letter, we demonstrate that the valley gap opening for low-lying LLs is the *intrinsic* property of graphene-like systems. These systems have a honeycomb crystallographic group that is different from the relativistic Lorenz group in QED albeit resulting in a similar Dirac-like equation for noninteracting fermions in zero magnetic field, $\boldsymbol{H} = 0$. The difference becomes apparent in an applied magnetic field when the additional translationally noninvariant terms accounting for interaction of microscopic intravalley and intervalley orbital currents with the magnetic field appear in the graphene Hamiltonian. The effect of the double-valley LL splitting has, therefore, a much more natural explanation as a *perturbative* noncritical orbital splitting that is of the same order as the standard Zeeman spin splitting.

We first consider the origin and symmetry properties of the Hamiltonian, the spectrum, and the wave functions of conducting electrons (holes) in the vicinity of two crystallographically nonequivalent opposite corners $\boldsymbol{K}_{1,2}$ (also denoted as $\boldsymbol{K}$ and $\boldsymbol{K}'$) of the hexagonal Brillouin Zone of graphene *at zero field*, $\boldsymbol{H} = 0$. The wave functions of the zero-energy states are located exactly at $\boldsymbol{K}_{1,2}$ and can be linearly expanded over a 4-component Bloch basis (irreducible representation) of the K point [25]:

$$\tilde{\Psi} \equiv \{\Psi_i\}_{i=1-4} = \{\Psi^A_{K_1}, \Psi^B_{K_1}, \Psi^B_{K_2}, \Psi^A_{K_2}\}^T \qquad (1)$$

(for symmetry reasons, our set $\{\Psi_i\}$ is different from the commonly used $\{\Psi^A_{K_1}, \Psi^B_{K_1}, \Psi^A_{K_2}, \Psi^B_{K_2}\}$).

TABLE I. Transformation properties of the Bloch spinor $\tilde{\Psi}$ ($\varepsilon = e^{2\pi i/3}$)

	C_6	σ_y	σ_x	$\hat{T}_{12}$
$\Psi^A_{K_1}$	$\bar{\varepsilon}\Psi^B_{K_2}$	$\Psi^A_{K_2}$	$\Psi^B_{K_1}$	$\varepsilon\Psi^A_{K_1}$
$\Psi^B_{K_1}$	$\varepsilon\Psi^A_{K_2}$	$\Psi^B_{K_2}$	$\Psi^A_{K_1}$	$\varepsilon\Psi^B_{K_1}$
$\Psi^A_{K_2}$	$\varepsilon\Psi^B_{K_1}$	$\Psi^A_{K_1}$	$\Psi^B_{K_2}$	$\bar{\varepsilon}\Psi^A_{K_2}$
$\Psi^B_{K_2}$	$\bar{\varepsilon}\Psi^A_{K_1}$	$\Psi^B_{K_1}$	$\Psi^A_{K_2}$	$\bar{\varepsilon}\Psi^B_{K_2}$

It is the transformation properties of spinorlike function $\tilde{\Psi}$ under the action of the graphene crystallographic group

$$G = \{C_6, C_3, C_2, \sigma_x, \sigma_y, R\} \times \{\boldsymbol{T}_1, \boldsymbol{T}_2\} \tag{2}$$

(Table I) that define all the physical properties of charge carriers in graphene. Here, $\boldsymbol{T}_{1,2}$ are the lattice translations; other notation is the same as in [25,26]. The physical properties can be obtained either directly from the standard Tables of Irreducible Representations of Crystallographic Groups [27] or from the explicit form of $\tilde{\Psi}$ in a tight-binding approximation of the carbon p_z orbitals marked as $\pi(\boldsymbol{r})$ (see also Fig. 1):

$$\Psi^{A(B)}_{K_{1,2}} = e^{(2\pi i/3)s_{A(B)}} \sum_{nm} e^{(2\pi i/3)s_{\boldsymbol{K}_{1,2}}(n+m)} \pi(\boldsymbol{r} - \boldsymbol{t}^{A(B)}_{nm}) \tag{3}$$

where $s_{A(B)} = +(-)1$, $s_{\boldsymbol{K}_{1,2}} = \pm 1$, and $\boldsymbol{t}^{A(B)}_{nm}$ are the A (B) sublattice coordinates indexed by $n, m = 0, \pm 1, \ldots$.

Wave functions of states deviating from $\boldsymbol{K}_{1,2}$ by a small vector $\boldsymbol{k} = (k_x, k_y)$ can also be expanded over the basis $\Psi_i(\boldsymbol{r})$, but with slowly space-varying envelopes $\tilde{F}^{\boldsymbol{k}} \equiv F^{\boldsymbol{k}}_i(\boldsymbol{r})$:

$$\Phi^{\boldsymbol{k}}(\boldsymbol{r}) = \sum_{i=1}^{4} F^{\boldsymbol{k}}_i(r)\Psi_i(\boldsymbol{r}). \tag{4}$$

The energy spectrum $E(\boldsymbol{k})$ and the corresponding envelope functions $\tilde{F}^{\boldsymbol{k}}(\boldsymbol{r})$ are the eigenvalues and eigenfunctions of the usual $\boldsymbol{K}\,\boldsymbol{k}$-perturbation equation:

$$\hat{H}\tilde{F}^{\boldsymbol{k}}(\boldsymbol{r}) = E(\boldsymbol{k})\tilde{F}^{\boldsymbol{k}}(\boldsymbol{r}) \tag{5}$$

where the $\boldsymbol{K}\,\boldsymbol{k}$-perturbation Hamiltonian,

$$\hat{H} = v\begin{pmatrix} 0 & \hat{k}_x + i\hat{k}_y & 0 & 0 \\ \hat{k}_x - i\hat{k}_y & 0 & 0 & 0 \\ 0 & 0 & 0 & -\hat{k}_x - i\hat{k}_y \\ 0 & 0 & -\hat{k}_x + i\hat{k}_y & 0 \end{pmatrix}, \tag{6}$$

where v is the (constant) Fermi velocity, $\hat{\boldsymbol{k}} = -i\hbar\boldsymbol{\nabla}$ was obtained as the most general 4×4 matrix that is linear in k and conserves the form $\langle\tilde{\Psi}\,\hat{H}\,\tilde{\Psi}\rangle$ under the action of the group G.

The Hamiltonian (6) has the structure of the relativistic Dirac Hamiltonian for massless fermions with a linear conical spectrum [Fig. 2(a)]:

$$E(\boldsymbol{k}) = \pm v|\boldsymbol{k}|, \tag{7}$$

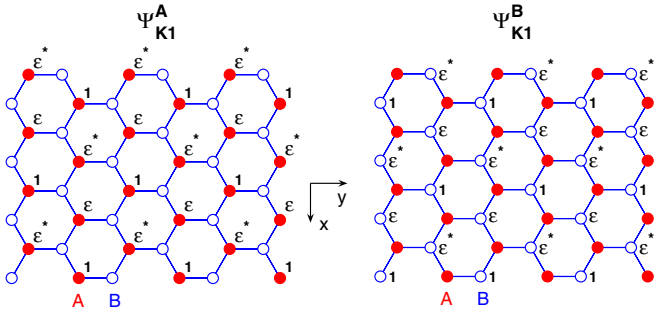

FIG. 1 (color online). K_1-point Bloch functions $\Psi^A_{K_1}$ and $\Psi^B_{K_1}$. The K_2-point Bloch functions $\Psi^A_{K_2}$ and $\Psi^B_{K_2}$ are obtained from them by applying complex conjugation.

and the corresponding system of eigenfunctions $\tilde{F}^{\boldsymbol{k}}(\boldsymbol{r})$ that is a linear superposition (with arbitrary complex constants c_1, c_2) of two-valley plane wave functions:

$$\tilde{F}^{\boldsymbol{k}}(\boldsymbol{r}) = c_1\{\pm e^{i\theta}, 1, 0, 0\}e^{i\vec{\boldsymbol{k}}\vec{\boldsymbol{r}}} + c_2\{0, 0, \mp e^{i\theta}, 1\}e^{i\vec{\boldsymbol{k}}\vec{\boldsymbol{r}}}, \tag{8}$$

where $\theta = \arctan(k_x/k_y)$ and the $\pm$ sign corresponds to the upper (lower) branch of the conical spectrum (7).

The Bloch expansion (4) also remains valid in a magnetic field $\boldsymbol{H}$, although the slowly varying coefficients $\tilde{F}(r)$ are now classified according to the discrete set of LLs (instead of continuous $\boldsymbol{k}$). The usual way of introducing $\boldsymbol{H} = \boldsymbol{\nabla} \times \boldsymbol{A}$ consists of the Peierls substitution

$$\hat{\boldsymbol{k}} \to \hat{\boldsymbol{k}} + \frac{|e|}{c}\boldsymbol{A}, \tag{9}$$

which in the case of the Hamiltonian (6) is the same as replacing $\hat{k}_x \pm i\hat{k}_y$ by the LL creation (annihilation) operators $a^{\pm}$.

The Hamiltonian has a set of discrete LLs having a square-root energy dependence on the level number $n = 0, \pm 1, \pm 2, \ldots$ in a magnetic field [Fig. 2(b)]:

$$E_n = s_{\mathrm{eh}}\sqrt{2v^2|e|\hbar H_z|n|/c}, \qquad s_{\mathrm{eh}} = \mathrm{sign}(n), \tag{10}$$

which is quite different from the case of massive particles with $E_n = \hbar\omega_c(n + \frac{1}{2}) \geq 0$, $(n = 0, 1, 2, \ldots)$, ω_c, the cyclotron frequency, and has solutions with values both above and below the zero-energy LL, $E_0 = 0$. The corresponding eigenfunctions can be written as an expansion over the nth LL eigenfunctions $f_n(r)$:

$$\tilde{F}^{n}(r) = \{c_1 f_{|n|}(r), s_{\mathrm{eh}} i c_1 f_{|n|-1}(r), \qquad c_2 f_{|n|}(r), s_{\mathrm{eh}} i c_2 f_{|n|-1}(r)\} \tag{11}$$

[note that $f_{-1}(r) \equiv 0$]. Each level, including $n = 0$, has the two-valley degeneracy provided by the complex constants c_1, c_2, the twofold spin degeneracy, and the infinite Landau degeneracy.

Although the Peierls substitution (9) conserves a relativistic invariance of the Dirac equation in a magnetic field, the discrete crystal lattice background leads to another, *weaker* requirement, that the Hamiltonian of the system should be invariant with respect to the crystallographic group of graphene in a magnetic field [26]:

$$G_H = \{C_6R, C_3, C_2R, \sigma_xR, \sigma_yR\}. \tag{12}$$

In particular, this time noninvariant group $G_H \subset G$ does

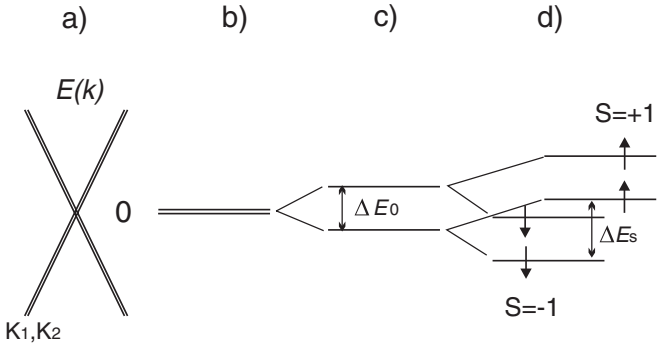

FIG. 2. (a) Two-valley degenerate Dirac-like spectrum $E(k)$ of charge carriers in zero magnetic field, $H = 0$. (b) Landau Level (LL) quantization of Dirac Fermions. (c) Orbital valley splitting of LLs. (d) Additional Zeeman spin splitting of LLs (only the $n = 0$ level is shown.)

not contain the translations $\boldsymbol{T}_{1,2}$, which are incompatible with the translational magnetic group.

The principal idea of the present work is that the graphene Hamiltonian for charge carriers in magnetic field should have a more general form:

$$\hat{H} = \begin{pmatrix} \lambda\mu_B H_z & va^+ & \gamma\mu_B H_z & 0 \\ va^- & -\lambda\mu_B H_z & 0 & -\gamma\mu_B H_z \\ \gamma\mu_B H_z & 0 & \lambda\mu_B H_z & -va^+ \\ 0 & -\gamma\mu_B H_z & -va^- & -\lambda\mu_B H_z \end{pmatrix} \quad (13)$$

($\mu_B = |e|\hbar/2mc$, where m is the bare electron mass) that, besides the Peierls terms $a^{\pm}$, contains the "nonrelativistic" λ- and γ- corrections provided by the orbital interaction of Bloch electrons with the magnetic field. These terms keep $\langle\tilde{\Psi}\hat{H}\tilde{\Psi}\rangle$ invariant under the operation of group G_H and are produced by the matrix elements:

$$\begin{aligned}\langle\Psi^A_{K_1}\hat{V}\bar{\Psi}^B_{K_2}\rangle &= -\langle\Psi^B_{K_1}\hat{V}\bar{\Psi}^A_{K_2}\rangle = \langle\Psi^B_{K_2}\hat{V}\bar{\Psi}^A_{K_1}\rangle \\ &= -\langle\Psi^A_{K_2}\hat{V}\bar{\Psi}^B_{K_1}\rangle = \gamma\mu_B H_z \end{aligned} \quad (14)$$

and

$$\begin{aligned}\langle\Psi^A_{K_1}\hat{V}\bar{\Psi}^A_{K_1}\rangle &= -\langle\Psi^B_{K_1}\hat{V}\bar{\Psi}^B_{K_1}\rangle = \langle\Psi^B_{K_2}\hat{V}\bar{\Psi}^B_{K_2}\rangle \\ &= -\langle\Psi^A_{K_2}\hat{V}\bar{\Psi}^A_{K_2}\rangle = \lambda\mu_B H_z \end{aligned} \quad (15)$$

of the perturbation operator

$$\hat{V} = -\boldsymbol{H}\cdot\boldsymbol{M} = -\frac{e}{2c}\boldsymbol{H}\cdot[\boldsymbol{r}\times\boldsymbol{v}], \quad (16)$$

that accounts for the translational-invariant symmetry breakdown due to the discrete crystal background [28,29]. (Analogous terms for the time-symmetry-breaking field have been proposed in [30] for the orbital part of intrinsic spin-orbit coupling in graphene, which is minute.) Using the expression for the velocity operator in the site representation, $\boldsymbol{v} = d\boldsymbol{r}/dt = i\hbar^{-1}[\hat{H},\boldsymbol{r}] = i\hbar^{-1}\sum t_{\pi\pi}\boldsymbol{\delta}|\boldsymbol{n}\rangle\times\langle\boldsymbol{n}+\boldsymbol{\delta}|$, where $\boldsymbol{\delta}$ is the vector connecting A and B sites in the graphene lattice (C-C interatomic distance $\delta =$ 1.42 Å), $\boldsymbol{n}$ the lattice vector, $t_{\pi\pi} = 3.033$ eV is the $\pi-\pi$ hopping integral. Now, we have for the cross product $[\boldsymbol{r}\times\boldsymbol{v}] = i\hbar^{-1}\sum t_{\pi\pi}[\boldsymbol{n}\times\boldsymbol{\delta}]|\boldsymbol{n}\rangle\langle\boldsymbol{n}+\boldsymbol{\delta}|$, and can estimate the parameter γ with the use of (14) and (16) as:

$$\gamma \approx \frac{t_{\pi\pi}/2}{\hbar^2/m\delta^2} = 0.4. \quad (17)$$

It is more difficult to estimate the next-nearest-neighbor parameter λ (between A and A') in (15), since the hopping integral falls off fairly slowly [$t_{\pi\pi}(d) \propto 1/d^2$] but, clearly, $\lambda < \gamma$.

Diagonalization of the Hamiltonian (13) can be easily done in terms of LL wave functions $f_n(r)$, presenting the resulting 4-component eigenfunctions $\tilde{F}^n(r)$ in the form (11) with slightly different coefficients. This again gives the set of discrete LLs with $n = 0, \pm1, \pm2, \ldots$, having the energies

$$E_n = s_{eh}\sqrt{2v^2|e|\hbar H_z|n|/c + \lambda^2\mu_B^2 H_z^2} \pm \gamma\mu_B H_z. \quad (18)$$

Special attention should be paid to zero LL $n = 0$ with

$$E_0 = (-\lambda \pm \gamma)\mu_B H_z \quad (19)$$

and

$$\tilde{F}^{\,0}_{\pm}(r) = \{f_0(r), 0, \pm f_0(r), 0\}. \quad (20)$$

The new effect here, illustrated by Fig. 2(c), is the valley splitting of each LL, marked by the $\pm$ sign

$$\Delta E_n = 2\gamma\mu_B H_z \approx 1.3\lambda H_z[\mathrm{T}]\mathrm{K}. \quad (21)$$

This splitting should be observable for zero LL in high fields. Note that this effect has purely orbital origin and is completely decoupled from the additional Zeeman spin-splitting shown in Fig. 2(d),

$$\Delta E_s \simeq g\mu_B H \simeq 1.3\frac{g}{2}H[\mathrm{T}]\mathrm{K}, \qquad g \approx 2, \quad (22)$$

because of very weak spin-orbital coupling. Unlike orbital splitting, the spin splitting is a function of the absolute value of $\boldsymbol{H}$ (rather than of H_z), that permits separating the two contributions ΔE_s and ΔE_n by their angular field dependence.

To clarify the physical origin of the orbital splitting, consider the explicit form of the wave functions for carriers located on the up or down shifted zero LL:

$$\Phi^0_{\pm}(\boldsymbol{r}) = \sum_{i=1}^{4} F^0_{i\pm}(\boldsymbol{r})\Psi_i(\boldsymbol{r}) = \Psi_{\pm}(\boldsymbol{r})f_0(\boldsymbol{r}), \quad (23)$$

where the Bloch parts,

$$\Psi_{\pm}(\boldsymbol{r}) = \Psi^A_{K_1}(\boldsymbol{r}) \pm \Psi^B_{K_2}(\boldsymbol{r}), \quad (24)$$

are shown in Fig. 3 and can be interpreted as a set of clockwise and counterclockwise closed current loops circulating around every third hexagon. (Some of the current loops appear nonclosed in Fig. 3, which is just a cutout from the infinite 2D graphene lattice. Nonclosed loops at

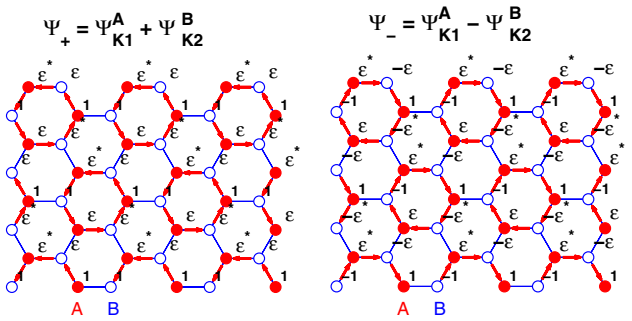

FIG. 3 (color online). Schematic of circular currents corresponding to Bloch functions $\Psi_{\pm} = \Psi^{A}_{K_1} \pm \Psi^{B}_{K_2}$ of the split zero Landau level.

the sample boundary are not allowed by current conservation.) Therefore, it is the orbital paramagnetic interaction of these *intervalley* circular currents with H_z that causes the splitting ΔE_0.

The current distribution for LLs with $n \neq 0$ is more complicated since both clockwise and counterclockwise current loops with different envelope LL functions [$f_n(r)$ and $f_{n-1}(r)$] contribute to the wave functions of each split LL. Note also that the additional contribution can be caused by the *intravalley* circular currents circulating around next-nearest-neighbor plaquettes proposed in [18]. Governed by the next-nearest-neighbor parameter λ, these currents do not contribute to LL splitting.

We have proven that the orbital mechanism is sufficient to explain the zero LL splitting in graphene. The effect occurs in a perturbative noncritical manner and is an intrinsic property of noninteracting fermions on a hexagonal lattice. As a consequence (observable, e.g., optically), the orbital splitting should not depend on the LL filling factor, unlike the result from other models. At the same time, the many-body and/or disorder effects can amplify the orbital splitting (even for $n \neq 0$), induce an additional symmetry breaking, and bring about a nontrivial field and filling factor dependence of the gap observed experimentally [11,12].

We thank Y. Kopelevich and M. Dyakonov for valuable discussions. I. L. was supported by ANR project LoMaCoQuP.

[1] I. A. Luk'yanchuk and Y. Kopelevich, Phys. Rev. Lett. **93**, 166402 (2004).
[2] K. S. Novoselov, A. K. Geim, and S. V. Morozov *et al.*, Nature (London) **438**, 197 (2005).
[3] Y. Zhang, Y.-W. Tan, H. L. Stormer, and P. Kim, Nature (London) **438**, 201 (2005).
[4] S. Y. Zhou, G.-H. Gweon, and J. Graf *et al.*, Nature Phys. **2**, 595 (2006).
[5] A. Bostwick, T. Ohta, and T. Seyller *et al.*, Nature Phys. **3**, 36 (2007).
[6] G. Li and E. Y. Andrei, Nature Phys. **3**, 623 (2007).
[7] Y. Kopelevich, J. H. S. Torres, and R. R. da Silva *et al.*, Phys. Rev. Lett. **90**, 156402 (2003).
[8] I. A. Luk'yanchuk and Y. Kopelevich, Phys. Rev. Lett. **97**, 256801 (2006).
[9] For a review, see: M. I. Katsnelson and K. S. Novoselov, Solid State Commun. **143**, 3 (2007).
[10] V. P. Gusynin and S. G. Sharapov, Phys. Rev. Lett. **95**, 146801 (2005).
[11] Y. Zhang, Z. Jiang, and J. P. Small *et al.*, Phys. Rev. Lett. **96**, 136806 (2006); Z. Jiang *et al.*, Phys. Rev. Lett. **99**, 106802 (2007).
[12] D. A. Abanin, K. S. Novoselov, and U. Zeitler *et al.*, Phys. Rev. Lett. **98**, 196806 (2007).
[13] For a review see K. Yang, Solid State Commun. **143**, 27 (2007).
[14] V. P. Gusynin, V. A. Miransky, and I. A. Shovkovy, Phys. Rev. Lett. **73**, 3499 (1994).
[15] H. A. Fertig and L. Brey, Phys. Rev. Lett. **97**, 116805 (2006).
[16] V. P. Gusynin, V. A. Miransky, S. G. Sharapov, and I. A. Shovkovy, Phys. Rev. B **74**, 195429 (2006).
[17] D. V. Khveshchenko, Phys. Rev. Lett. **87**, 206401 (2001); **87**, 246802 (2001).
[18] J. Alicea and M. P. A. Fisher, Phys. Rev. B **74**, 075422 (2006).
[19] J.-N. Fuchs and P. Lederer, Phys. Rev. Lett. **98**, 016803 (2007).
[20] K. Nomura and A. H. MacDonald, Phys. Rev. Lett. **96**, 256602 (2006).
[21] M. O. Goerbig, R. Moessner, and B. Douçot, Phys. Rev. B **74**, 161407 (2006).
[22] D. A. Abanin, P. A. Lee, and L. S. Levitov, Phys. Rev. Lett. **98**, 156801 (2007).
[23] A. H. Castro Neto, F. Guinea, and N. M. R. Peres, Phys. Rev. B **73**, 205408 (2006).
[24] D. A. Abanin, P. A. Lee, and L. S. Levitov, Phys. Rev. Lett. **96**, 176803 (2006).
[25] L. D. Landau and E. M. Lifshitz, *Statistical Physics* (Butterworth-Heinemann, Oxford, 1984), Part 1.
[26] L. D. Landau and E. M. Lifshitz, *Electrodynamics of Continuous Media* (Butterworth-Heinemann, Oxford, 1985).
[27] O. V. Kovalev, *Presentation of Crystallographic Space Groups: Irreducible Representations, Induced Representations, and Corepresentations* (CRC Press, New York, 1993).
[28] E. M. Lifshitz and L. P. Pitaevskii, *Statistical Physics* (Butterworth-Heinemann, Oxford, 2002), Part 2.
[29] E. I. Blount, Phys. Rev. **126**, 1636 (1962).
[30] J. L. Mañes, F. Guinea, and M. A. H. Vozmediano, Phys. Rev. B **75**, 155424 (2007).